

Article

The Molecular Mechanism of circRNA-11228/miR-103/INSIG1 Pathway Regulating Milk Fat Synthesis in Bovine Mammary Epithelial Cells

Xiaofen Li ^{1,*}, Yanni Wu ², Yuhao Wang ², Xiaozhi Yang ¹, Rui Gao ², Qinyue Lu ³, Xiaoyang Lv ^{4,5} and Zhi Chen ²

¹ School of Animal Science and Technology, Jiangsu Agri-Animal Husbandry Vocational College, Taizhou 225300, China

² College of Animal Science and Technology, Yangzhou University, Yangzhou 225009, China; mx120220877@stu.yzu.edu.cn (Y.W.); mx120220872@stu.yzu.edu.cn (Y.W.); mx1202308812@stu.yzu.edu.cn (R.G.); zhichen@yzu.edu.cn (Z.C.)

³ Laboratory of Animal Developmental Biology, Department of Animal Science, Chungbuk National University, Cheongju 28644, Republic of Korea; surpassroad@163.com

⁴ Joint International Research Laboratory of Agriculture & Agri-Product Safety, Ministry of Education, Yangzhou University, Yangzhou 225009, China; dx120170085@yzu.edu.cn

⁵ International Joint Research Laboratory in Universities of Jiangsu Province of China for Domestic Animal Germplasm Resources and Genetic Improvement, Yangzhou 225009, China

* Correspondence: lxf@jshvc.edu.cn

Abstract: Milk, known for its high content of short- and medium-chain fatty acids and unsaturated fatty acids, has attracted substantial attention due to its nutritional and health value. The regulation of fatty acid metabolism by non-coding RNAs has become a subject of growing attention, particularly in relation to fatty acid production at the transcriptional/epigenetic and post-transcriptional levels. This study established the circRNA-11228/miR-103/INSIG1 (insulin-inducible gene) regulatory network using methods such as qRT-PCR, dual luciferase reporting, and Western blot, with INSIG1 serving as the starting point. The experimental validation of circRNA-11228's impact on cholesterol levels, lipid droplet secretion, and unsaturated fatty acid content was conducted using various assays, including triglycerides, cholesterol, oil red O, and EdU(5-ethynyl-2'-deoxyuridine) in bovine mammary epithelial cells (BMECs). Furthermore, the transfection of mimics and inhibitors synthesized from miR-103 into BMECs confirmed that miR-103 can promote cholesterol synthesis and lipid droplet secretion. Conversely, the INSIG1 gene was found to inhibit cholesterol synthesis and lipid droplet secretion. The "remediation" experiment validated the ability of miR-103 to alleviate the cellular effect of circRNA-11228. Taken together, our findings indicate that the binding of circRNA-11228 to miR-103 inhibits the expression of the target gene INSIG, thereby regulating milk fat production in BMECs. This study offers novel insights into producing high-quality milk and new ways to improve the dietary composition of residents.

Keywords: circRNA-11228; miR-103; INSIG1; bovine mammary epithelial cells; milk fat synthesis



Citation: Li, X.; Wu, Y.; Wang, Y.; Yang, X.; Gao, R.; Lu, Q.; Lv, X.; Chen, Z. The Molecular Mechanism of circRNA-11228/miR-103/INSIG1 Pathway Regulating Milk Fat Synthesis in Bovine Mammary Epithelial Cells. *Agriculture* **2024**, *14*, 538. <https://doi.org/10.3390/agriculture14040538>

Academic Editors: Michael Schutz and Fangxiang Shi

Received: 15 January 2024

Revised: 26 January 2024

Accepted: 27 March 2024

Published: 28 March 2024



Copyright: © 2024 by the authors. Licensee MDPI, Basel, Switzerland. This article is an open access article distributed under the terms and conditions of the Creative Commons Attribution (CC BY) license (<https://creativecommons.org/licenses/by/4.0/>).

1. Introduction

In recent times, circular RNAs (circRNAs) have garnered scholarly attention as a type of non-coding RNAs (ncRNAs) [1,2]. Despite being initially observed under electron microscopy in 1979, circRNAs have predominantly been considered as byproducts of RNA splicing and thus have received limited attention due to their low abundance and insufficient functional research. However, recent advances in RNA sequencing, quantitative PCR, and computational analysis methods have revealed their widespread occurrence and specific expressions in tissues. Due to their long half-life, circRNAs become a key post-transcriptional regulator of genes by binding to microRNAs and relieving their inhibition of mRNA targets. Moreover, they also exert an influence on gene expressions at the

transcriptional level. Although the biological mechanism of circRNAs remains elusive, it is widely accepted that the majority of circRNAs are generated by the conventional splicing mechanism through head-to-tail dorsal splicing [3]. Interestingly, milk fat contains approximately 14% of active transcriptional genes capable of producing circRNAs, indicating that RNA cyclization is a prevalent cellular attribute. Extensive studies have shown that circRNAs are emerging as a pivotal regulatory factor affecting diverse domains of life, such as lactation, development, differentiation, and disease-related biological processes. For example, circRNAs can interact with transcription factors and RNA-binding proteins (RBPs) to form ribonucleoprotein complexes with specific functions [4]. Additionally, they can form RNA-RNA complexes with non-coding RNAs (such as lncRNAs) and mRNAs [5]. These hybrid RNA complexes can alter the function or stability of these RNA molecules, while circRNA mRNA complexes possess the ability to influence the stability or translation of mRNAs [6,7]. In this study, insulin-inducible gene1 (INSIG1), which has already been functionally defined, was chosen as the research object. Through sequence analysis, *INSIG1* was determined to contain a binding site for miR-103, and another binding site was also identified between circRNA-11228 and miR-103. Given the close association between INSIG and cholesterol metabolism, it is speculated that circRNA-11228/miR-103/INSIG1 may exert a regulatory effect on milk fat cholesterol synthesis. However, further research is needed to investigate the regulatory role of circRNA-11228, its regulatory mechanism, and the regulatory factors that respond to it.

INSIG1, a member of the INSIG family, is a transmembrane protein consisting of six domains embedded in the endoplasmic reticulum membrane [8,9]. Its encoded protein participates in regulating intracellular lipid metabolism homeostasis by modulating the activation of sterol regulatory element-binding proteins (SREBPs) and the degradation of 3-hydroxy-3-methylglutaryl CoA reductase (HMGCR) [10,11]. A growing number of experimental and clinical evidence indicates that INSIG1 possesses the ability to reduce lipid accumulation in liver cells, thereby alleviating the progression of non-alcoholic fatty liver disease, lowering plasma free cholesterol levels, and subsequently protecting against β . The absence of fat toxicity in cells contributes to the mitigation of abnormal blood lipid levels in individuals with diabetes. In addition, the inhibitory effects of INSIG1 on adipogenesis and precursor adipocyte differentiation play a crucial role in preventing obesity [12]. Therefore, INSIG1 can serve as a key regulatory factor in maintaining intracellular lipid metabolism homeostasis, making it a promising therapeutic target for lipid disorders [13]. Despite the increasing interest among researchers, there is still a limited understanding of the regulatory relationship between INSIG1 and its upstream factors, especially in the context of circRNA regulation.

MicroRNAs (miRNAs) can regulate multiple target genes, while individual genes can also be regulated by diverse miRNAs [14,15]. The critical role of miRNAs in cellular processes, such as cell proliferation, apoptosis, lipid and protein synthesis, and body metabolism, is attributed to their regulation of various signaling pathway molecules [16]. In order to investigate this phenomenon, a group of researchers constructed miRNA expression profiles in breast tissues of mice, goats, and cows at different lactation stages and conducted a comprehensive analysis of these profiles. Their findings revealed significant differences in miRNA expression profiles across these stages. The differential expression of miRNAs is hypothesized to be related to breast development and lactation-related milk fat metabolism activities [17]. In the mouse 3T3-L1 cell line, miR-103 has been found to promote intracellular triglyceride synthesis by targeting the *MEF2D* (myocyte enhancer factor 2D) gene and activating the AKT/mTOR signaling pathway [18,19]. Moreover, the expression level of miR-199-3p in human adipocytes is influenced by free fatty acids, insulin resistance, and inflammatory factors, making it a potential marker for fatty acid content [20]. The aforementioned studies provide compelling evidence that miRNAs play an important role in animal fatty acid metabolism. Bioinformatics analysis has discovered that the 5' untranslated region (5'-UTR) of the *INSIG1* gene contains a binding site for miR-103. However, limited reports exist regarding the regulatory relationship between miR-

103 and INSIG1. Therefore, we hypothesized that the circRNA-11228/miR-103 pathway might regulate lipid compositions via competitively binding INSIG1 in bovine mammary epithelial cells (BMECs). To test the hypothesis, various molecular biological techniques and functional experiments, such as gene overexpression, dual-luciferase reporter vectors, and Western blotting, were employed to further evaluate the function and regulatory relationship of circRNA-11228/miR-103/INSIG1.

2. Materials and Methods

2.1. Culture of BMECs (Bovine Mammary Epithelial Cells)

Cows selected in this study were 60 days postpartum (peak lactation) Holstein cows (body weight: 650 ± 50 kg) and daily milk yields (40 ± 5 kg), and in vivo udder tissues were collected surgically. After washing with PBS (phosphate-buffered saline), visible adipose tissues and connective tissues surrounding the breast tissue were removed. The remaining tissues were then placed in a frozen tube containing D-Hank's solution and kept on ice before transporting them to the laboratory. Tissue block separation was used to separate BMECs. The acinus structure was cut from the tissue block and finely shredded into cubes of approximately 1 mm^3 . Then, they were placed in a pre-soaked culture dish containing serum and cultured with 5% CO_2 at 37°C . The culture medium was replaced every 2–3 days. Upon migration of cells from the tissue block, they were digested for passage. Following passage culture, breast epithelial cells were purified using differential digestion and frozen. BMECs were cultured in a complete growth medium consisting of DMEM-F12, 10% fetal bovine serum (FBS, Wisent, Nanjing, China), and 50 U/mL penicillin streptomycin in a 37°C 5% CO_2 incubator for subsequent experiments.

2.2. Triglycerides and Cholesterol Analysis

Once the treated cells reached a fusion degree of 90–100%, they were collected, and the culture medium was discarded from the culture plate. Subsequently, the cells were washed three times with pre-cooled PBS at 4°C and then subjected to ice lysis for 20 min using the lysate. Then, a cell scraper was used to scrape the cells and lysate into a centrifuge tube, followed by sonication. After standing on ice for 10 min and fully crushing, the sample was centrifuged at 2000 rpm at 4°C for 5 min. Following centrifugation, a portion of the supernatant was extracted, and the total protein concentration was determined using the BCA (bicinchoninic acid assay) protein detection kit. The remaining supernatant was heated at 70°C for 10 min, followed by centrifugation at 2000 rpm for 5 min at room temperature. To ascertain the concentration of triglycerides or cholesterol, the reaction was shielded from light for 10 min and subsequently carried out for 20 min. The blank control group was set up simultaneously, and the absorbance at 550 nm was employed to detect intracellular concentrations of triglycerides or cholesterol. Based on the measurement results, a standard curve was drawn and the concentration of triglycerides was calculated. Triglyceride content was quantified using protein concentration per milligram. For specific methods, please refer to Chen et al. [21,22].

2.3. Oil Red O Staining

Cells were inoculated into a 12-well plate, followed by the removal of the culture medium and gentle rinsing of the cells twice with pre-cooled PBS buffer. Subsequently, the cells were fixed with 4% paraformaldehyde at room temperature for 30 min. The fixative was then removed, and cells were rinsed twice with pre-cooled PBS buffer. Then, cells were stained with oil red O working solution at room temperature for 30 min. The oil red O working solution was discarded, and cells were gently rinsed twice with pre-cooled PBS buffer. Then, cells were stained with hematoxylin staining solution in the dark for 3 min. Following this, the hematoxylin staining solution was discarded and cells were rinsed twice with pre-cooled PBS buffer. Then, a fluorescence microscope was employed to observe and take photos.

2.4. EdU Cell Proliferation Detection

Cells were inoculated into a 24-well plate and diluted in a ratio of EdU (10 mM) to growth medium 1:500 to obtain 2× of EdU working solution (20 μM). After preheating at 37 °C, the same volume of culture medium was added to a 24-well plate. The final concentration of EdU was reduced to 1×, and the plate was placed in a cell incubator for further cultivation for 6 h. Next, the culture medium was removed and 500 μL of 4% paraformaldehyde was added, allowing for fixation at room temperature for 15 min. The fixed solution was then removed, and each well was incubated with 500 μL PBS buffer at room temperature for 15 min. Hoechst 33342 (1000×) was diluted with PBS buffer at a ratio of 1:1000. Then, 100 μL 1× Hoechst 33342 was added to each well, followed by incubation at room temperature in darkness for 10 min to facilitate nuclear staining. Subsequently, the staining solution was removed. Fluorescence detection was conducted using a fluorescence microscope.

2.5. Double Luciferase Report

After digestion, 293A cells were inoculated into a 48-well plate, with an approximate density of 7×10^4 cells per well. After 24 h, the state and density of 293A cells were observed. Once 293A cells stably adhered to the wall and reached a density of 75%, the reporter gene plasmid vector was transferred into them through PEI (polyethyleneimine) transfection reagent. After 4 h, the fluorescence was observed using a fluorescence microscope. After 48 h, the cells were washed 3 times with PBS, followed by treatment with 40 μL of 1× passive lysis buffer. The resulting mixture was then shaken for 15 min using a shaker, after which the liquid was collected in a 1.5 mL EP (Eppendorf) tube and centrifuged for 10 min at 3500 rpm. From the resulting supernatant, 4 μL was taken for detection and mixed with 20 μL Mix LARII well. Then, the fluorescence value was measured using Lumit3 LB9508, and 20 μL of Stop & Go solution was added. The experimental data were subsequently analyzed and normalized to obtain fluorescence report detection results. To verify the targeting relationship, PCDNA-miR-103 was co-transfected with recombinant psiCHECK-2-circ003429-W/psiCHECK-2-circ003429-Mut vector into HEK293T cells, and dual-luciferase gene reporter vector test was employed.

2.6. Quantitative Real-Time PCR (qRT-PCR)

To detect mRNA expression levels, mRNA reverse transcription fluorescence quantitative PCR (qRT-PCR) was employed following the protocols provided by the PrimeScriptTM reverse transcription kit and TB GreenTM quantitative PCR kit. The relative expression levels of genes were calculated by UXT (ubiquitously expressed prefoldin-like chaperone) as an internal reference. The purpose and quantitative PCR primers for internal reference genes can be found in Supplementary Materials (Table S1).

The detection of miRNA through reverse transcription fluorescence quantitative PCR involved diluting the cDNA by a factor of 10, ensuring the thorough mixing of the reaction system. Following this, it was pre-denatured at 95 °C for 3 min in the CFX-96 real-time fluorescence quantitative PCR instrument. Subsequently, PCR amplification was performed at 60 °C for 30 s following a 10-s denaturation at 95 °C, with a total of 40 cycles. The relative expression levels of miRNA were quantitatively calculated using 18S rRNA as an internal reference.

2.7. Western Blot

The culture medium was discarded, and the cells were gently rinsed with pre-cooled PBS buffer. Cells were then treated with 4 °C pre-cooled RIPA cracking solution and cleaved on ice for 30 min. Next, the lysate was transferred into a centrifuge tube and centrifuged at 10,000 rpm for 10 min. The supernatant was collected, and the protein concentration was determined using the BCA reagent kit. The denatured protein was subjected to SDS-PAGE (dodecyl sulfate, sodium salt-polyacrylamide gel electrophoresis) electrophoresis and transferred onto the PVDF (polyvinylidene fluoride) membrane, which

was then sealed with a blocking solution. Following the instructions provided by the antibody, antibodies specific to the target gene were used. The first antibody was incubated overnight at 4 °C, and the second antibody was incubated in darkness for 1.5 h at room temperature. ECL (electrogenenerated chemiluminescence) luminescent liquid was prepared and used in conjunction with a chemiluminescence imaging system to detect the intensity of the protein signal.

2.8. Data Analysis

The data were presented using the mean ± standard deviation. Statistical analysis was conducted using SPSS 19.0 software, particularly through two-tailed F-tests and one-way ANOVA, to compare and analyze the differences between groups. All experiments were duplicated and repeated three times. The results are expressed as the means ± standard errors. Differences were considered significant at * $p < 0.05$; ** $p < 0.01$.

3. Results

3.1. Targeting *INSIG1* with miR-103 Specificity

The online software TargetScan 6.2 was utilized to identify that miR-103 exhibited a perfect match with its target gene 3'-UTR, and it is suggested that *INSIG1* may serve as the target gene for miR-103. Our findings also revealed that the overexpression of miR-103 led to a downregulation of the *INSIG1* gene, while inhibition of miR-103 resulted in the upregulation of mRNA expression levels of the *INSIG1* gene (Figure 1A). Similarly, the protein expression and mRNA expression trends of *INSIG1* remained consistent under the overexpression and inhibition of miR-103 (Figure 1B). The 3'-UTR of the *INSIG1* gene was bound to the miR-103 site (Figure 1C). Luciferase reporter gene analysis showed that the overexpression of miR-103 downregulated the activity of the wild-type *INSIG1* gene 3'-UTR, while the activity of the *INSIG1* gene in the mutant remained unchanged (Figure 1D).

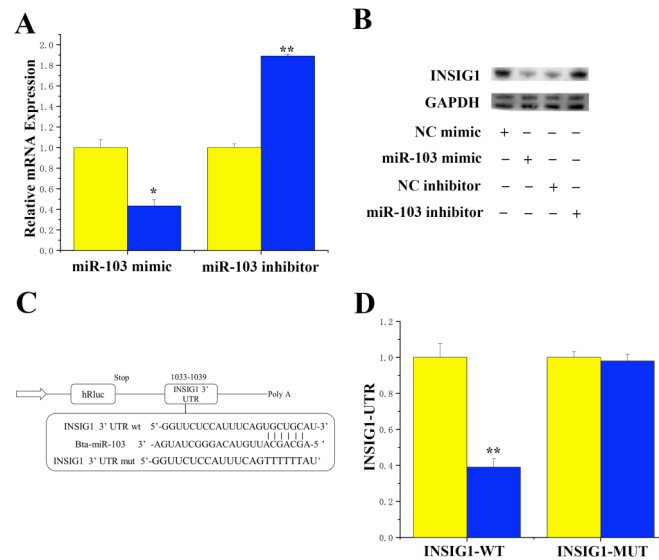


Figure 1. Targeting *INSIG1* with miR-103 specificity. (A) The effect of miR-103 mimic and inhibitor on the expression level of *INSIG1* mRNA. Yellow bars: negative control; blue bars: miR-103 mimic or inhibitor. (B) The effect of miR-103 mimic and inhibitor on *INSIG1* protein levels. (C) Analysis of binding sites of miR-103 on *INSIG1* 3'-UTR. (D) The effect of miR-103 on the activity of *INSIG1* gene 3'-UTR wild-type and mutant luciferase reporter vectors. WT: a luciferase reporter vector containing wild-type *INSIG1* 3'-UTR (1033 bp to 1039 bp); MUT: a mutant luciferase reporter vector containing the miR-103-binding site on *INSIG1* 3'-UTR. Yellow bars: negative control; blue bars: miR-103 mimic. All experiments were duplicated and repeated three times. Values are presented as means ± standard errors, * $p < 0.05$, ** $p < 0.01$. Significant differences * or ** compare the variables studied (blue bars) with their negative controls (yellow bars)?

3.2. CircRNA-11228 Competitive Binding to miR-103

Sequence analysis demonstrated that circRNA-11228 originated from a specific region on chromosome X between 90989590 and 90994621. Additionally, the circRNA-11228 sequence was found to contain a miR-103-binding site. To verify the potential binding between circRNA-11228 and miR-103, we employed PCR to amplify and recombine the sequence containing the miR-103-binding site into the psiCHECK-2 vector to form a wild-type recombinant vector. Furthermore, we introduced mutations to the binding site by overlapping PCR to generate a mutant psiCHECK-2 vector (Figure 2A, Table S2). To determine whether circRNA-11228 possesses the ability to target miR-103, we conducted a dual-luciferase reporter gene assay. The results showed a significant decrease ($p < 0.05$) in activity subsequent to the co-transfection of miR-103 with wild-type vectors (comparison between yellow and blue), whereas no substantial change in activity was observed with mutant vectors compared to the control group (Figure 2B, comparison between yellow and green). Moreover, circRNA-11228 significantly reduced ($p < 0.01$) the expression of miR-103 (Figure 2C), indicating its ability to adsorb and bind to miR-103.

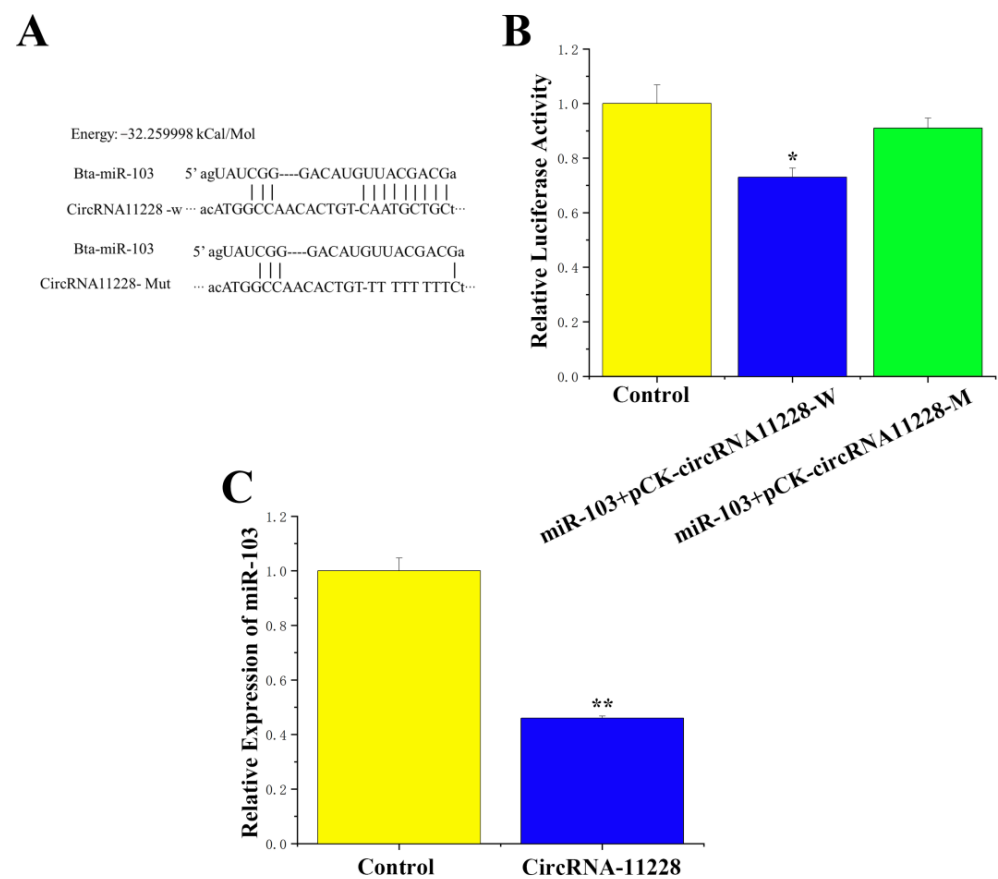


Figure 2. CircRNA-11228 competitive binding miR-103. (A) The potential binding site between circRNA-11228 and miR-103. (B) MiR-103 mimic reduces the activity of pCK circRNA-11228 luciferase. (C) CircRNA-11228 reduces the expression of miR-103. All experiments were duplicated and repeated three times. Values are presented as means \pm standard errors, * $p < 0.05$, ** $p < 0.01$.

3.3. Transfection Efficiency of circRNA-11228, miR-103, and siRNA INSIG1

In order to determine the function of circRNA-11228 in BMECs, an overexpression vector containing the circRNA-11228 sequence (pcDNA circRNA11228, Tables S3 and S4) was constructed. After transfection with the overexpression vector, it was observed that the overexpression efficiency of circRNA-11228 increased by 18 times (Figure 3A), indicating that its overexpression can be used for subsequent studies. The expression levels of miR-103 in the miR-103 mimic treatment group were approximately 37.5 times higher than that in

the control group, whereas these levels were downregulated by about 70% in the group treated with miR-103 inhibitor. This finding demonstrated that the transfection efficiency of miR-103 mimic and inhibitor was substantial, rendering them suitable for experiments (Figure 3B). The transfection of SiRNA-INSIG1 resulted in a significant downregulation ($p < 0.01$) of intracellular INSIG1 expression of over 60% (Figure 3C).

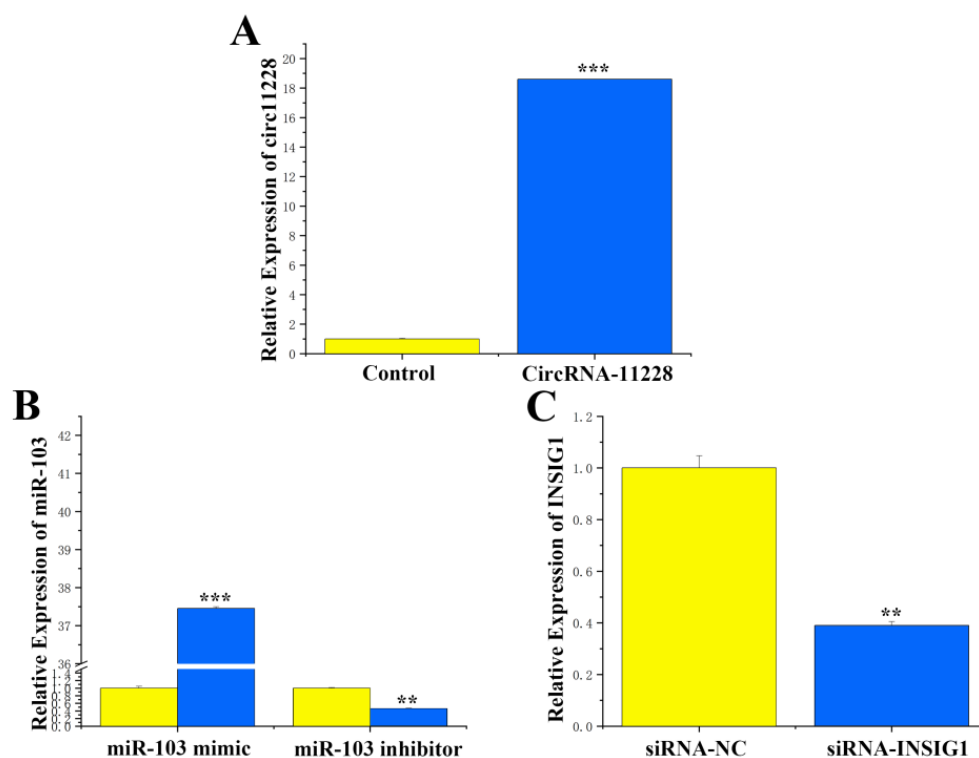


Figure 3. Transfection efficiency of circRNA-11228, miR-103, and siRNA-INSIG1 in BMECs. (A) Detection of circRNA-11228 after transfection with pcDNA-circRNA11228. (B) Detection of miR-103 after transfection with miR-103 mimic/inhibitor. Yellow bars: negative control; blue bars: miR-103 mimic or inhibitor. (C) Detection of *INSIG1* after transfection with siRNA-INSIG1. All experiments were duplicated and repeated three times. Values are presented as means \pm standard errors, ** $p < 0.01$, *** $p < 0.001$. Significant differences ** or *** compare the variables studied (blue bars) with their negative controls (yellow bars).

3.4. Functional Validation of circRNA-11228 in BMECs

We detected levels of triglycerides, cholesterol, and lipid droplet secretion in response to the overexpression of circRNA-11228. The findings showed significant decreases ($p < 0.05$) in triglyceride levels (Figure 4A) and cholesterol levels (Figure 4B). On the other hand, oil red O staining results revealed that the circRNA-11228 overexpression substantially reduced lipid droplet accumulation of BMECs (Figure 5A). The EdU assay results demonstrated that overexpression of circRNA-11228 did not lead to a decrease in cell count (Figure 5B). Concurrently, examination of the expression levels of genes related to milk fat metabolism demonstrated a substantial downregulation of cholesterol transport genes (ABCA1 (ATP-binding cassette subfamily A member 1) and ABCG1 (ATP-binding cassette subfamily G member 1)), triglyceride-synthesis-related genes (ACACA (acetyl-CoA carboxylase alpha), SCD (stearoyl-CoA desaturase), and DGAT1 (diacylglycerol O-acyltransferase 1)), lipid droplet formation-related genes (ADRP (PLIN2)) (Figure 4C), and fatty acid synthesis-related genes (FASN (fatty acid synthase) and ACSS1 (acyl-CoA synthetase short-chain family member 1)) (Figure 4D), whereas upregulation of lipolysis-related genes (HSL (homo sapiens)) and oxidation-related genes (ACSL1 (acyl-CoA synthetase long-chain family member 1) and ACOX (acyl-CoA oxidase 1)) (Figure 4E).

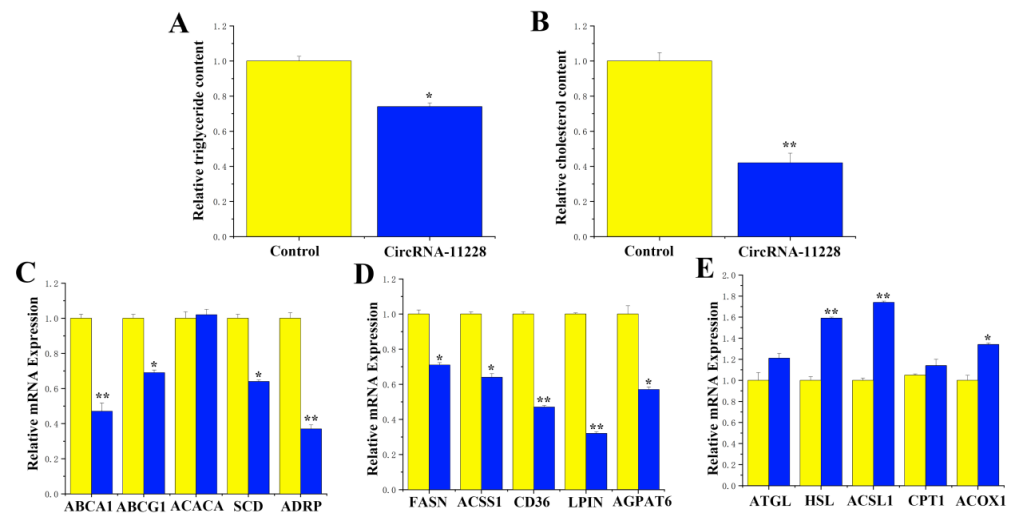


Figure 4. Functional validation of circRNA-11228 in BMECs. (A) The level of triglyceride synthesis in BMECs treated with circRNA-11228. (B) The level of cholesterol in BMECs treated with circRNA-11228. (C–E) The effect of circRNA-11228 on the expression level of genes related to milk fat metabolism. Yellow bars: negative control; blue bars: overexpression of circRNA-11228. * $p < 0.05$, ** $p < 0.01$. All experiments were duplicated and repeated three times. Values are presented as means \pm standard errors, * $p < 0.05$, ** $p < 0.01$. Significant differences * or ** compare the variables studied (blue bars) with their negative controls (yellow bars).

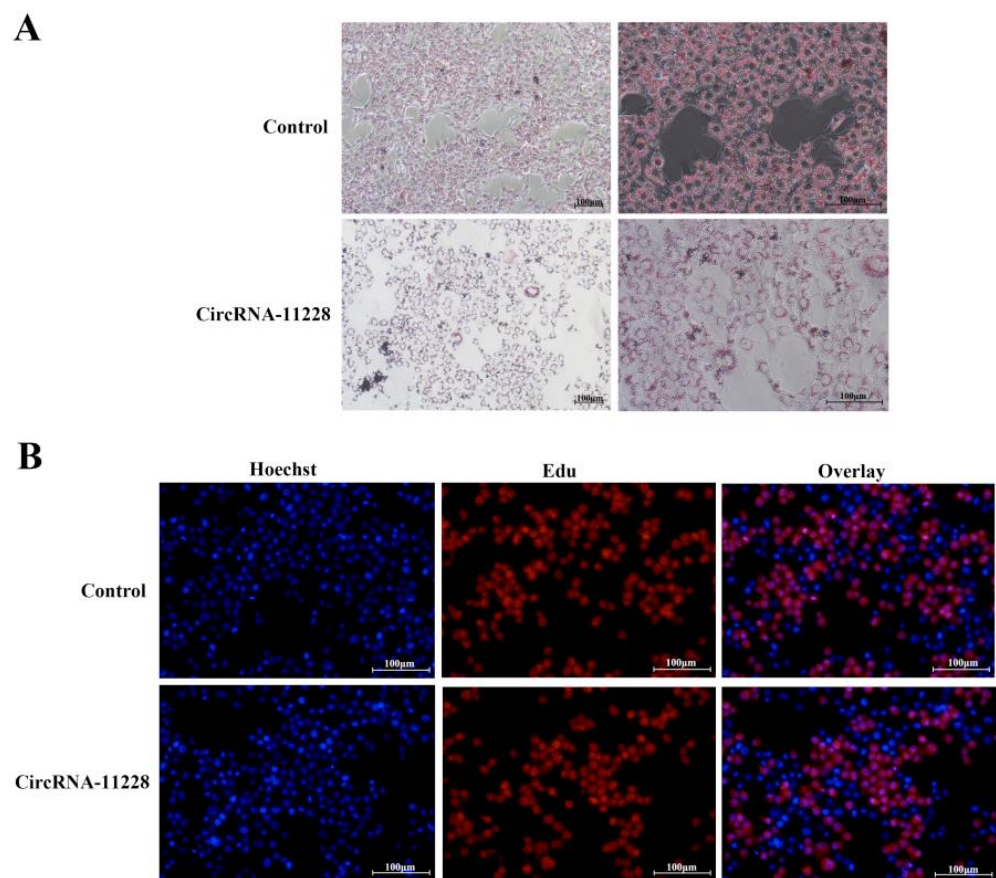


Figure 5. Lipid droplet secretion and differentiation of circRNA-11228 in BMECs. (A) The accumulation of lipid droplets dealt with circRNA-11228 in BMECs. (B) Cell differentiation dealt with circRNA-11228 in BMECs.

3.5. Functional Validation of miR-103 in BMECs

The results revealed that inhibiting miR-103 expression significantly reduced ($p < 0.05$) triglyceride content (Figure 6A). Conversely, overexpression of miR-103 resulted in an approximately 1.7-fold increase in cholesterol concentration (Figure 6B). Additionally, inhibiting miR-103 led to a 0.7-fold reduction in cholesterol content, whereas miR-103 mimics significantly increased ($p < 0.01$) intracellular lipid droplet accumulation in BMECs (Figure 6C).

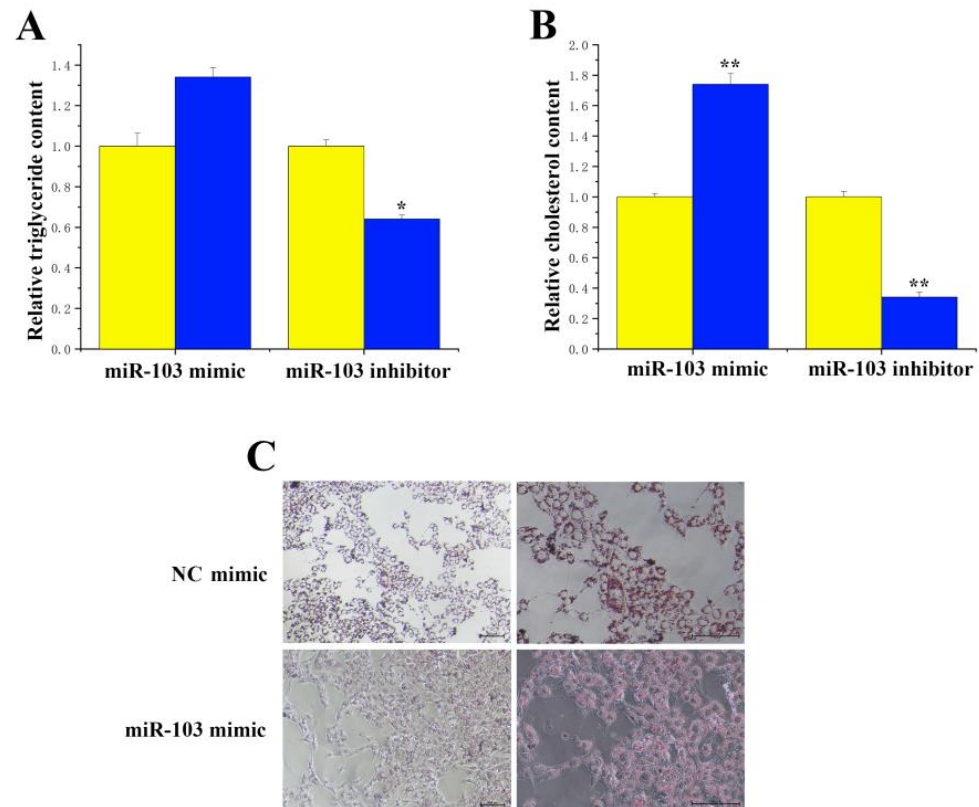


Figure 6. Functional validation of miR-103 in BMECs. (A) The level of triglyceride synthesis in BMECs treated with miR-103. Yellow bars: negative control; blue bars: miR-103 mimic or inhibitor. (B) The level of cholesterol in BMECs treated with circRNA-11228. Yellow bars: negative control; blue bars: miR-103 mimic or inhibitor. (C) The accumulation of lipid droplets in BMECs treated with miR-103 mimic. All experiments were duplicated and repeated three times. Values are presented as means \pm standard errors, * $p < 0.05$, ** $p < 0.01$. Significant differences * or ** compare the variables studied (blue bars) with their negative controls (yellow bars).

3.6. Functional Validation of INSIG1 in BMECs

Levels of triglycerides, cholesterol concentration, and lipid droplet secretion in cells were evaluated in response to siRNA-INSIG1 treatment in cells. Compared with the control group, the concentration of triglycerides in BMECs was upregulated albeit not significantly (Figure 7A). Conversely, we detected a more than 1.7-fold increase in the cholesterol content (Figure 7B). Meanwhile, we employed oil red O staining and found that siRNA-INSIG1 promoted fat droplet formation (Figure 7C).

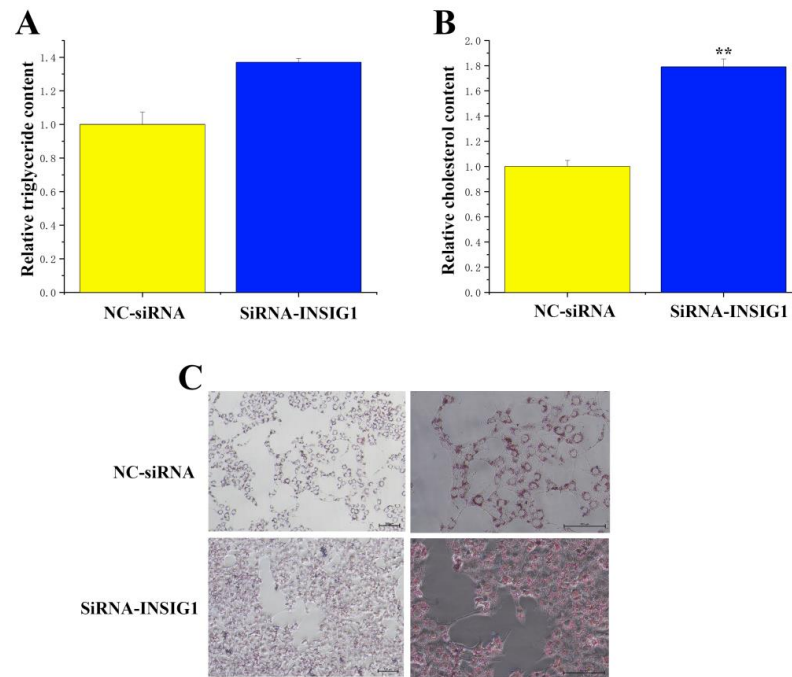


Figure 7. Functional validation of *INSIG1* in BMECs. (A) The level of triglyceride synthesis in BMECs treated with siRNA-*INSIG1*. (B) The level of cholesterol in BMECs treated with siRNA-*INSIG1*. (C) The accumulation of lipid droplets in BMECs treated with siRNA-*INSIG1*. All experiments were duplicated and repeated three times. Values are presented as means \pm standard errors ** $p < 0.01$.

3.7. *CircRNA-11228* Regulates Cholesterol Metabolism in BMECs by Adsorbing *miR-133a*

CircRNA-11228 was found to diminish cholesterol levels in BMECs, and this reduction was mitigated upon treatment with *miR-103* (Figure 8A). In addition, we detected the expression level of the *INSIG1* gene in response to the overexpression of *circRNA-11228*. The results revealed that *circRNA-11228* significantly enhanced ($p < 0.05$) the mRNA expression of the *INSIG1* gene. Moreover, *miR-103* significantly declined *INSIG1* gene expression. When cells were treated with *circRNA-11228* + *miR-103*, the expression level of *INSIG1* did not change (Figure 8B).

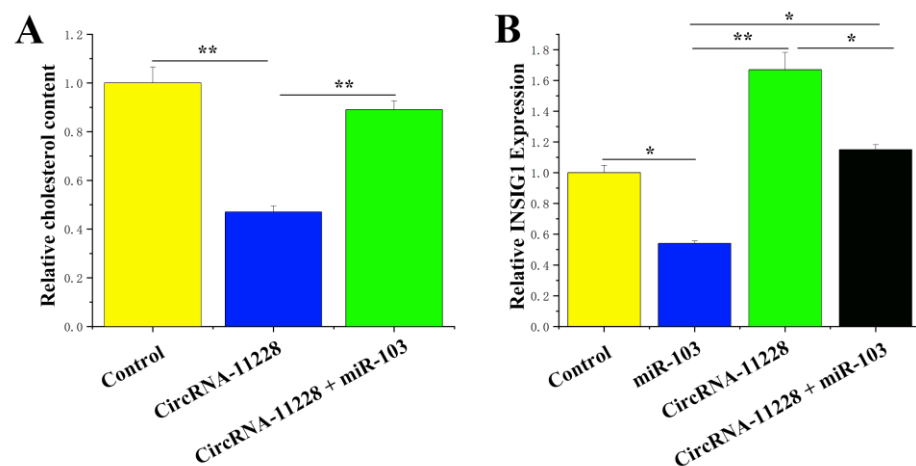


Figure 8. *CircRNA-11228* promotes cholesterol metabolism in BMECs by adsorbing *miR-103*. (A) TAG levels in cells transfected with control, *circRNA-11228*, or *circRNA-11228* + *miR-103*. (B) *INSIG1* expression levels in cells transfected with control, *miR-103*, *circ007071*, and *circRNA-11228* + *miR-103*. All experiments were duplicated and repeated three times. Values are presented as means \pm standard errors, * $p < 0.05$, ** $p < 0.01$.

4. Discussion

The acylation reaction of glycerol-3-phosphate serves as the initial stage in the biosynthesis of glycerol lipid, which is catalyzed by GPAM (glycerol-3-phosphate acyltransferase, mitochondrial) [23,24]. The reduction in cellular triglyceride content by *INSIG1* may be attributed to the inhibitory effect of *INSIG1* on the expression levels of GPAM gene mRNA. The activation of AMPK (adenosine 5'-monophosphate (AMP)-activated protein kinase) can induce the phosphorylation of many proteins, thereby increasing glucose uptake and metabolism and promoting fatty acid oxidation, while concurrently inhibiting liver adipogenesis, cholesterol synthesis, and glucose production [25]. The elevated expression of *INSIG1* may be responsible for the general increase in saturated fatty acid, monounsaturated fatty acid, and polyunsaturated fatty acid content in cells. This effect could potentially be attributed to the presence of AMPK α 1, which is encoded by *PRKAA1* (protein kinase AMP-activated catalytic subunit alpha 1) and functions as a cell energy sensor [26,27]. Activation of AMPK α 1 also deactivates energy-consuming processes such as fatty acid biosynthesis, while simultaneously activating production processes such as fatty acid oxidation. Consequently, the expression of the *INSIG1* gene can cause changes in gene expression closely related to lipid metabolism, including leptin, *SCD*, *FASN*, and *HSL*. These findings strongly suggest that the *INSIG1* gene is a functional gene that significantly influences lipid metabolism. Additionally, both *INSIG1* and *FASN* genes have been identified as target genes for miR-24 in mice and goats [28–30]. By transfecting siRNA to interfere with the *INSIG1* gene, we observed that interfering with the *INSIG1* gene in miR-24 knockout cells can partially reverse the decrease in lipid droplets, triglycerides, and cholesterol content caused by miRNA knockout. This investigation serves as the initial validation of the regulatory relationship between miR-103 and *INSIG1*, demonstrating the specific targeting of *INSIG1* by miR-103. Consequently, this study establishes a fundamental basis for subsequent in vivo experiments.

MiRNAs are a class of short-stranded, non-coding RNAs that exert their regulatory effects by inducing degradation and inhibiting translation of target genes through specific binding to 3'-UTR. A growing body of studies has demonstrated their regulatory roles in various biological processes [14,15], including cell proliferation [31], differentiation [32], apoptosis [33], and so on. In addition, it has been observed that a single miRNA may target multiple genes, thereby exerting a multifaceted impact [34]. For instance, miR-143 [35], miR-369-5p [36], and miR-27b [37,38] have been implicated in adipocyte differentiation processes. It can be seen that the investigation of miRNAs holds considerable significance in elucidating the molecular mechanisms underlying fat metabolism. The oil red O staining and EdU results of this study demonstrate that miR-103 enhances the accumulation of lipid droplets in BMECs without affecting cell proliferation. This indicates that miR-103 primarily promotes intracellular secretion of lipid droplets rather than stimulating cell proliferation.

Intracellular fatty acids mainly contribute to the formation of triglycerides, which are stored in cells [39]. Triglycerides and cholesterol jointly participate in the formation of intracellular lipid components [40]. The promotion of cholesterol and triglyceride levels, together with circRNA-11228, may be attributed to *ABCA1* and *ABCG1* responsible for cholesterol transport, as well as *ACACA*, *SCD*, and *DGAT1* responsible for triglyceride synthesis. Lipid droplets, consisting of triglycerides and cholesterol encapsulated in phospholipid monolayers, are synthesized and secreted through the participation of *ADFP*, *XDH*, and *TIP47* genes. *ACACA* catalyzes the conversion of acetyl CoA to malonyl CoA, a rate-limiting enzyme for the synthesis of C16:0 fatty acids from scratch [41,42]. The potential mechanism by which circRNA-11228 inhibits the upregulation of C16:0 and C18:0 fatty acid content in BMECs may involve the co-regulatory effect of intracellular *ELOVL6* and *SCD1* proteins.

When studying the function of circRNA, it is crucial to consider its expression abundance in relation to its linear RNA copies (mRNA or lncRNA). Although most circRNAs are generally less abundant than linear RNAs, there are instances where circRNAs ex-

hibit higher levels of abundance [43,44]. The competitive binding between circRNAs and miRNAs can affect the translation and/or stability of mRNAs [1,2,4,15,31]. In addition, circRNAs can directly interact with various RNA molecules such as mRNAs and lncRNAs [1,4,45], influencing their stability, translation, and localization [44]. For example, the formation of a loop by mRNA can lead to an enhancement of its translation efficiency due to the proximity facilitated by circRNAs between the 5' and 3' ends of the target mRNA, thereby affecting mRNA translation. Additionally, circRNAs can also interact with RBPs and even function as RBP sponges. Through their interaction with RBPs, circRNAs may affect the splicing, transportation, storage, and translation of target mRNAs. On the contrary, the binding of RBPs to mRNAs can exert an influence on the formation, function, abundance, and subcellular localization of circRNAs [46]. It is worth noting that despite the recognized stability of circRNAs, their turnover remains unexplored in response to changes in RBP levels that interact with it. Similarly, the interaction between circRNAs and transcription factors (TF) can affect TF translocation to the nucleus or transcriptional activity. For example, circ-Foxo3 can serve as bait for TF. Notably, research has described that circRNA-11228 promotes cholesterol and fatty acids by adsorbing miR-103. Through software prediction and a dual luciferase reporter gene detection system, the binding between circRNA-11228 and miR-103 has been experimentally proven. Interestingly, circRNA-11228 and miR-103 exhibit completely opposing effects on the metabolism of cholesterol and fatty acids. Specifically, circRNA-11228 inhibits their metabolism, while the overexpression of miR-103 can counteract this effect. In addition, circRNA-1128 has been observed to inhibit milk fat metabolism, and this effect can be reversed when miR-103 is overexpressed. Also, circRNA-1128 has been determined to decrease triglyceride synthesis. However, when circRNA-1128 and miR-103 are overexpressed concurrently, the triglyceride levels are not different from those of the control group. These results indicate that circRNA-1128 functions as a molecular sponge of miR-103.

5. Conclusions

Our data reveal that during the dry milk period of cows, circRNA-11228 binds to miR-103, thereby alleviating the inhibitory effect of miR-103 on *INSIG1* expression. On the other hand, after lactation in cows, circRNA-11228 did not interfere with miR-103's specific targeting of *INSIG1*; *INSIG1* does not have an effect on milk fat metabolism (Figure 9). These findings provide a solid theoretical and experimental basis for comprehending molecular mechanisms underlying the regulation of milk fat synthesis.

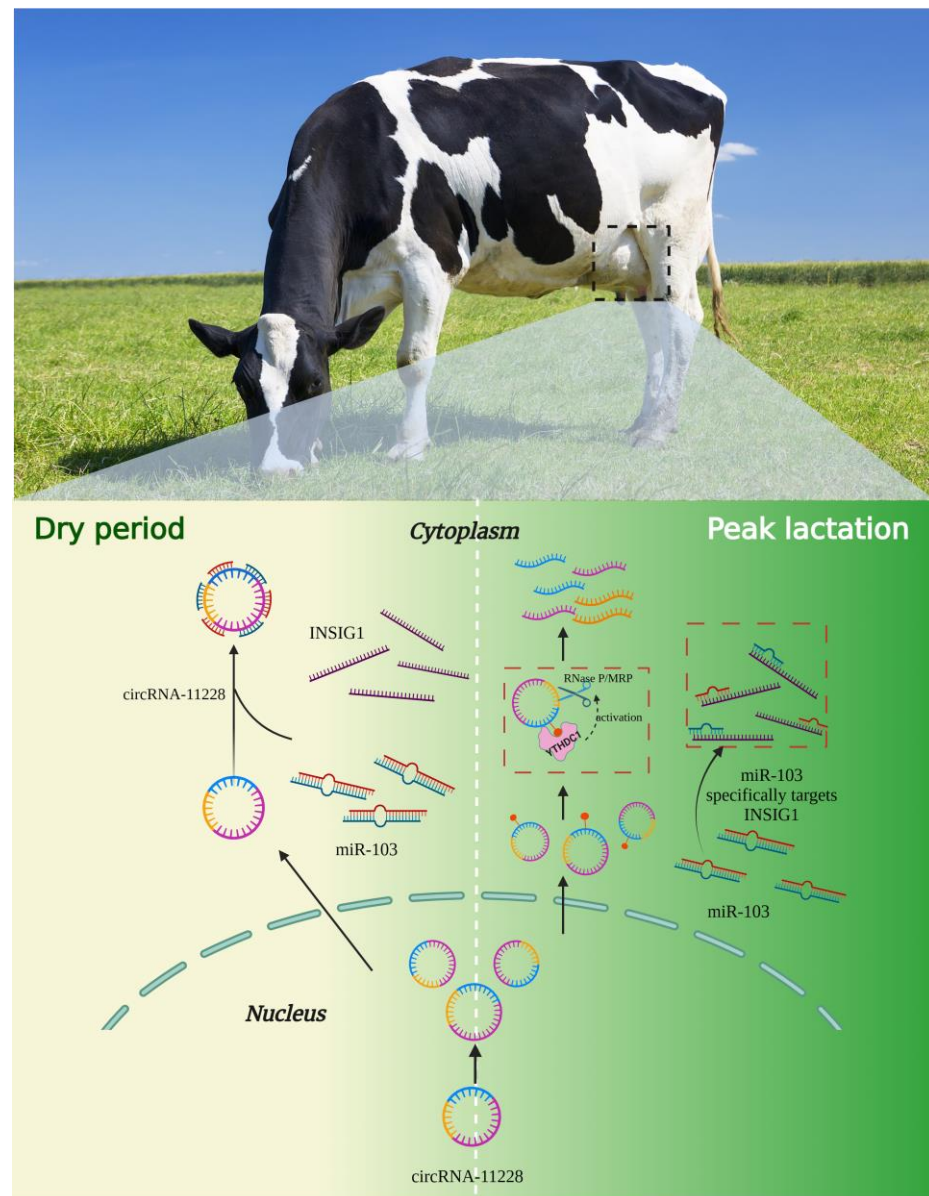


Figure 9. The molecular mechanism of circRNA-11228/miR-103/INSIG1 pathway regulating milk fat synthesis in BMECs.

Supplementary Materials: The following supporting information can be downloaded at <https://www.mdpi.com/article/10.3390/agriculture14040538/s1>, Table S1: Primer sequence of genes; Table S2: Mutant vector sequence; Table S3: CircRNA_11228 sequence; Table S4: pcDNA-circRNA11228 primer sequence.

Author Contributions: Conceptualization, Z.C. and X.L. (Xiaofen Li); methodology, Y.W. (Yanni Wu) and Y.W. (Yuhao Wang); formal analysis, X.Y. and R.G.; investigation: Q.L.; resources, Z.C. and X.L. (Xiaofen Li); writing—original draft preparation, Z.C. and X.L. (Xiaofen Li); writing—review and editing, X.L. (Xiaofen Li); supervision, X.L. (Xiaoyang Lv); project administration, Z.C. All authors have read and agreed to the published version of the manuscript.

Funding: This study was supported by Taizhou Science and Technology Support Plan (Agriculture) Project (TN202313) and the National Natural Science Foundation of China (Grant Nos. 32272825), the Open Project Program of the International Joint Research Laboratory of the Universities of Jiangsu Province of China for Domestic Animal Germplasm Resources and Genetic Improvement (IJRLD-KF202210), and Independent Innovation in Jiangsu Province of China (CX (21) 3119); “Qing Lan Project” and the “High-end talent support program” of Yangzhou University, China.

Institutional Review Board Statement: Not applicable.

Data Availability Statement: The original contributions presented in the study are included in the article/Supplementary Material.

Conflicts of Interest: We certify that there are no conflicts of interest with any financial organization regarding the material discussed in the manuscript.

References

1. Beermann, J.; Piccoli, M.T.; Viereck, J.; Thum, T. Non-coding RNAs in Development and Disease: Background, Mechanisms, and Therapeutic Approaches. *Physiol. Rev.* **2016**, *96*, 1297–1325. [[CrossRef](#)] [[PubMed](#)]
2. Zhou, W.Y.; Cai, Z.R.; Liu, J.; Wang, D.S.; Ju, H.Q.; Xu, R.H. Circular RNA: Metabolism, functions and interactions with proteins. *Mol. Cancer* **2020**, *19*, 172. [[CrossRef](#)] [[PubMed](#)]
3. Abe, B.T.; Wesselhoeft, R.A.; Chen, R.; Anderson, D.G.; Chang, H.Y. Circular RNA migration in agarose gel electrophoresis. *Mol. Cell* **2022**, *82*, 1768–1777.e1763. [[CrossRef](#)] [[PubMed](#)]
4. Amaya, L.; Grigoryan, L.; Li, Z.; Lee, A.; Wender, P.A.; Pulendran, B.; Chang, H.Y. Circular RNA vaccine induces potent T cell responses. *Proc. Natl. Acad. Sci. USA* **2023**, *120*, e2302191120. [[CrossRef](#)] [[PubMed](#)]
5. Xiao, Y.; Tang, Z.; Huang, X.; Chen, W.; Zhou, J.; Liu, H.; Liu, C.; Kong, N.; Tao, W. Emerging mRNA technologies: Delivery strategies and biomedical applications. *Chem. Soc. Rev.* **2022**, *51*, 3828–3845. [[CrossRef](#)] [[PubMed](#)]
6. Liu, X.; Zhang, Y.; Zhou, S.; Dain, L.; Mei, L.; Zhu, G. Circular RNA: An emerging frontier in RNA therapeutic targets, RNA therapeutics, and mRNA vaccines. *J. Control Release* **2022**, *348*, 84–94. [[CrossRef](#)]
7. Hill, M.; Tran, N. miRNA:miRNA Interactions: A Novel Mode of miRNA Regulation and Its Effect on Disease. *Adv. Exp. Med. Biol.* **2022**, *1385*, 241–257.
8. Smith, E.M.; Zhang, Y.; Baye, T.M.; Gawrieh, S.; Cole, R.; Blangero, J.; Carless, M.A.; Curran, J.E.; Dyer, T.D.; Abraham, L.J.; et al. INSIG1 influences obesity-related hypertriglyceridemia in humans. *J. Lipid Res.* **2010**, *51*, 701–708. [[CrossRef](#)] [[PubMed](#)]
9. Xu, D.; Wang, Z.; Xia, Y.; Shao, F.; Xia, W.; Wei, Y.; Li, X.; Qian, X.; Lee, J.H.; Du, L.; et al. The gluconeogenic enzyme PCK1 phosphorylates INSIG1/2 for lipogenesis. *Nature* **2020**, *580*, 530–535. [[CrossRef](#)] [[PubMed](#)]
10. Xu, Y.; Tao, J.; Yu, X.; Wu, Y.; Chen, Y.; You, K.; Zhang, J.; Getachew, A.; Pan, T.; Zhuang, Y.; et al. Hypomorphic ASGR1 modulates lipid homeostasis via INSIG1-mediated SREBP signaling suppression. *JCI Insight* **2021**, *6*, e147038. [[CrossRef](#)]
11. Cheng, C.; Ru, P.; Geng, F.; Liu, J.; Yoo, J.Y.; Wu, X.; Cheng, X.; Euthine, V.; Hu, P.; Guo, J.Y.; et al. Glucose-Mediated N-glycosylation of SCAP Is Essential for SREBP-1 Activation and Tumor Growth. *Cancer Cell* **2015**, *28*, 569–581. [[CrossRef](#)] [[PubMed](#)]
12. Azzu, V.; Vacca, M.; Kamzolas, I.; Hall, Z.; Leslie, J.; Carobbio, S.; Virtue, S.; Davies, S.E.; Lukasik, A.; Dale, M.; et al. Suppression of insulin-induced gene 1 (INSIG1) function promotes hepatic lipid remodelling and restrains NASH progression. *Mol. Metab.* **2021**, *48*, 101210. [[CrossRef](#)] [[PubMed](#)]
13. Fan, X.; Qiu, L.; Teng, X.; Zhang, Y.; Miao, Y. Effect of INSIG1 on the milk fat synthesis of buffalo mammary epithelial cells. *J. Dairy Res.* **2020**, *87*, 349–355. [[CrossRef](#)] [[PubMed](#)]
14. Zhu, L.; Jiao, H.; Gao, W.; Huang, L.; Shi, C.; Zhang, F.; Wu, J.; Luo, J. Fatty Acid Desaturation Is Suppressed in Mir-26a/b Knockout Goat Mammary Epithelial Cells by Upregulating INSIG1. *Int. J. Mol. Sci.* **2023**, *24*, 10028. [[CrossRef](#)] [[PubMed](#)]
15. Lu, T.X.; Rothenberg, M.E. MicroRNA. *J. Allergy Clin. Immunol.* **2018**, *141*, 1202–1207. [[CrossRef](#)] [[PubMed](#)]
16. Saliminejad, K.; Khorram Khorshid, H.R.; Soleymani Fard, S.; Ghaffari, S.H. An overview of microRNAs: Biology, functions, therapeutics, and analysis methods. *J. Cell Physiol.* **2019**, *234*, 5451–5465. [[CrossRef](#)] [[PubMed](#)]
17. Fabian, M.R.; Sonenberg, N.; Filipowicz, W. Regulation of mRNA translation and stability by microRNAs. *Annu. Rev. Biochem.* **2010**, *79*, 351–379. [[CrossRef](#)] [[PubMed](#)]
18. Ding, J.; Xia, C.; Cen, P.; Li, S.; Yu, L.; Zhu, J.; Jin, J. MiR-103-3p promotes hepatic steatosis to aggravate nonalcoholic fatty liver disease by targeting of ACOX1. *Mol. Biol. Rep.* **2022**, *49*, 7297–7305. [[CrossRef](#)] [[PubMed](#)]
19. Li, M.; Liu, Z.; Zhang, Z.; Liu, G.; Sun, S.; Sun, C. miR-103 promotes 3T3-L1 cell adipogenesis through AKT/mTOR signal pathway with its target being MEF2D. *Biol. Chem.* **2015**, *396*, 235–244. [[CrossRef](#)]
20. Wang, Z.; Shen, W.; Zhu, M.; Xu, M.; Qiu, M.; Zhang, D.; Chen, S. MiR-199-3p Suppressed Inflammatory Response by Targeting MECP2 to Alleviate TRX-Induced PHN in Mice. *Cell Transplant.* **2022**, *31*, 9636897221108192. [[CrossRef](#)]
21. Chen, Z.; Lu, Q.; Liang, Y.; Cui, X.; Wang, X.; Mao, Y.; Yang, Z. Circ11103 Interacts with miR-128/PPARGC1A to Regulate Milk Fat Metabolism in Dairy Cows. *J. Agric. Food Chem.* **2021**, *69*, 4490–4500. [[CrossRef](#)] [[PubMed](#)]
22. Chen, Z.; Lu, Q.; Zhang, X.; Zhang, Z.; Cao, X.; Wang, K.; Lu, X.; Yang, Z.; Loo, J.J.; Jiao, P. Circ007071 Inhibits Unsaturated Fatty Acid Synthesis by Interacting with miR-103-5p to Enhance PPAR γ Expression in the Dairy Goat Mammary Gland. *J. Agric. Food Chem.* **2022**, *70*, 13719–13729. [[CrossRef](#)] [[PubMed](#)]
23. Sveinbjornsson, G.; Ulfarsson, M.O.; Thorolfsson, R.B.; Jonsson, B.A.; Einarsson, E.; Gunnlaugsson, G.; Rognvaldsson, S.; Arnar, D.O.; Baldvinsson, M.; Bjarnason, R.G.; et al. Multiomics study of nonalcoholic fatty liver disease. *Nat. Genet.* **2022**, *54*, 1652–1663. [[CrossRef](#)] [[PubMed](#)]
24. Li, F.; Li, D.; Zhang, M.; Sun, J.; Li, W.; Jiang, R.; Han, R.; Wang, Y.; Tian, Y.; Kang, X.; et al. miRNA-223 targets the GPAM gene and regulates the differentiation of intramuscular adipocytes. *Gene* **2019**, *685*, 106–113. [[CrossRef](#)] [[PubMed](#)]

25. Han, Y.; Hu, Z.; Cui, A.; Liu, Z.; Ma, F.; Xue, Y.; Liu, Y.; Zhang, F.; Zhao, Z.; Yu, Y.; et al. Post-translational regulation of lipogenesis via AMPK-dependent phosphorylation of insulin-induced gene. *Nat. Commun.* **2019**, *10*, 623. [[CrossRef](#)] [[PubMed](#)]
26. Yang, Q.; Xu, J.; Ma, Q.; Liu, Z.; Sudhakar, V.; Cao, Y.; Wang, L.; Zeng, X.; Zhou, Y.; Zhang, M.; et al. PRKAA1/AMPK α 1-driven glycolysis in endothelial cells exposed to disturbed flow protects against atherosclerosis. *Nat. Commun.* **2018**, *9*, 4667. [[CrossRef](#)] [[PubMed](#)]
27. Yang, Q.; Ma, Q.; Xu, J.; Liu, Z.; Mao, X.; Zhou, Y.; Cai, Y.; Da, Q.; Hong, M.; Weintraub, N.L.; et al. Endothelial AMPK α 1/PRKAA1 exacerbates inflammation in HFD-fed mice. *Br. J. Pharmacol.* **2022**, *179*, 1661–1678. [[CrossRef](#)] [[PubMed](#)]
28. Huang, L.; Luo, J.; Gao, W.; Song, N.; Tian, H.; Zhu, L.; Jiang, Q.; Loo, J.J. CRISPR/Cas9-Induced Knockout of miR-24 Reduces Cholesterol and Monounsaturated Fatty Acid Content in Primary Goat Mammary Epithelial Cells. *Foods* **2022**, *11*, 2012. [[CrossRef](#)] [[PubMed](#)]
29. Ng, R.; Wu, H.; Xiao, H.; Chen, X.; Willenbring, H.; Steer, C.J.; Song, G. Inhibition of microRNA-24 expression in liver prevents hepatic lipid accumulation and hyperlipidemia. *Hepatology* **2014**, *60*, 554–564. [[CrossRef](#)]
30. Chen, C.; Wang, S.; Zhang, M.; Chen, B.; You, C.; Xie, D.; Liu, Y.; Monroig, Ó.; Tocher, D.R.; Waiho, K.; et al. miR-24 is involved in vertebrate LC-PUFA biosynthesis as demonstrated in marine teleost *Siganus canaliculatus*. *Biochim. Biophys. Acta Mol. Cell Biol. Lipids* **2019**, *1864*, 619–628. [[CrossRef](#)]
31. Rodriguez, R.E.; Schommer, C.; Palatnik, J.F. Control of cell proliferation by microRNAs in plants. *Curr. Opin. Plant Biol.* **2016**, *34*, 68–76. [[CrossRef](#)] [[PubMed](#)]
32. Shao, X.; Gong, W.; Wang, Q.; Wang, P.; Shi, T.; Mahmut, A.; Qin, J.; Yao, Y.; Yan, W.; Chen, D.; et al. Atrophic skeletal muscle fibre-derived small extracellular vesicle miR-690 inhibits satellite cell differentiation during ageing. *J. Cachexia Sarcopenia Muscle* **2022**, *13*, 3163–3180. [[CrossRef](#)] [[PubMed](#)]
33. Song, Y.; Zhang, C.; Zhang, J.; Jiao, Z.; Dong, N.; Wang, G.; Wang, Z.; Wang, L. Localized injection of miRNA-21-enriched extracellular vesicles effectively restores cardiac function after myocardial infarction. *Theranostics* **2019**, *9*, 2346–2360. [[CrossRef](#)] [[PubMed](#)]
34. Krol, J.; Loedige, I.; Filipowicz, W. The widespread regulation of microRNA biogenesis, function and decay. *Nat. Rev. Genet.* **2010**, *11*, 597–610. [[CrossRef](#)] [[PubMed](#)]
35. Liu, J.; Wang, H.; Zeng, D.; Xiong, J.; Luo, J.; Chen, X.; Chen, T.; Xi, Q.; Sun, J.; Ren, X.; et al. The novel importance of miR-143 in obesity regulation. *Int. J. Obes.* **2023**, *47*, 100–108. [[CrossRef](#)]
36. Bork, S.; Horn, P.; Castoldi, M.; Hellwig, I.; Ho, A.D.; Wagner, W. Adipogenic differentiation of human mesenchymal stromal cells is down-regulated by microRNA-369-5p and up-regulated by microRNA-371. *J. Cell Physiol.* **2011**, *226*, 2226–2234. [[CrossRef](#)] [[PubMed](#)]
37. Benito-Vicente, A.; Uribe, K.B.; Rotllan, N.; Ramírez, C.M.; Jebari-Benslaiman, S.; Goedeke, L.; Canfrán-Duque, A.; Galicia-García, U.; Saenz De Urturi, D.; Aspichueta, P.; et al. miR-27b Modulates Insulin Signaling in Hepatocytes by Regulating Insulin Receptor Expression. *Int. J. Mol. Sci.* **2020**, *21*, 8675. [[CrossRef](#)] [[PubMed](#)]
38. Sakai, E.; Imaizumi, T.; Suzuki, R.; Taracena-Gándara, M.; Fujimoto, T.; Sakurai, F.; Mizuguchi, H. miR-27b targets MAIP1 to mediate lipid accumulation in cultured human and mouse hepatic cells. *Commun. Biol.* **2023**, *6*, 669. [[CrossRef](#)]
39. Generoso, G.; Janovsky, C.; Bittencourt, M.S. Triglycerides and triglyceride-rich lipoproteins in the development and progression of atherosclerosis. *Curr. Opin. Endocrinol. Diabetes Obes.* **2019**, *26*, 109–116. [[CrossRef](#)]
40. McKenzie, K.M.; Lee, C.M.; Mijatovic, J.; Haghighi, M.M.; Skilton, M.R. Medium-Chain Triglyceride Oil and Blood Lipids: A Systematic Review and Meta-Analysis of Randomized Trials. *J. Nutr.* **2021**, *151*, 2949–2956. [[CrossRef](#)]
41. Peng, J.Y.; Cai, D.K.; Zeng, R.L.; Zhang, C.Y.; Li, G.C.; Chen, S.F.; Yuan, X.Q.; Peng, L. Upregulation of Superenhancer-Driven LncRNA FASRL by USF1 Promotes De Novo Fatty Acid Biosynthesis to Exacerbate Hepatocellular Carcinoma. *Adv. Sci.* **2022**, *10*, e2204711. [[CrossRef](#)] [[PubMed](#)]
42. Zheng, Z.G.; Zhu, S.T.; Cheng, H.M.; Zhang, X.; Cheng, G.; Thu, P.M.; Wang, S.P.; Li, H.J.; Ding, M.; Qiang, L.; et al. Discovery of a potent SCAP degrader that ameliorates HFD-induced obesity, hyperlipidemia and insulin resistance via an autophagy-independent lysosomal pathway. *Autophagy* **2021**, *17*, 1592–1613. [[CrossRef](#)] [[PubMed](#)]
43. Liu, C.X.; Chen, L.L. Circular RNAs: Characterization, cellular roles, and applications. *Cell* **2022**, *185*, 2016–2034. [[CrossRef](#)] [[PubMed](#)]
44. Wen, S.Y.; Qadir, J.; Yang, B.B. Circular RNA translation: Novel protein isoforms and clinical significance. *Trends Mol. Med.* **2022**, *28*, 405–420. [[CrossRef](#)] [[PubMed](#)]
45. Li, X.; Yang, L.; Chen, L.L. The Biogenesis, Functions, and Challenges of Circular RNAs. *Mol. Cell* **2018**, *71*, 428–442. [[CrossRef](#)]
46. Belousova, E.A.; Filipenko, M.L.; Kushlinskii, N.E. Circular RNA: New Regulatory Molecules. *Bull. Exp. Biol. Med.* **2018**, *164*, 803–815. [[CrossRef](#)]

Disclaimer/Publisher’s Note: The statements, opinions and data contained in all publications are solely those of the individual author(s) and contributor(s) and not of MDPI and/or the editor(s). MDPI and/or the editor(s) disclaim responsibility for any injury to people or property resulting from any ideas, methods, instructions or products referred to in the content.